

Growth phenomena on C₆₀ crystals

M.A. Verheijen, W.J.P. van Enckevort and G. Meijer

Research Institute for Materials, Faculty of Science, University of Nijmegen, Toernooiveld, 6525 ED Nijmegen, The Netherlands

Received 22 September 1993

The {111} and {100} faces of C₆₀ crystals grown from the vapour phase have been studied by phase sensitive optical microscopy. On these faces growth steps, dislocation outcrops, epitaxial dendrites, slip lines and cracks have been observed, their occurrence depending on the crystal face and on the growth conditions.

1. Introduction

Since Krätschmer et al. [1] described a method for synthesizing fullerenes in macroscopic amounts, a lot of research has been performed, especially on C₆₀. Crystals of C₆₀ have been grown from various solutions as well as from the vapour phase [1–5]. Growth from solutions results in different crystal structures, depending on the solvent used and on the amount of solvent incorporated into the crystal lattice. By growth from the vapour phase one is able to obtain solvent free crystals of relatively good crystallographic perfection, which have the fcc crystal structure.

The size of the C₆₀ molecules (7 Å cage diameter) enables observation of low (monomolecular) growth layers on a crystal surface by atomic force microscopy (AFM) and by phase sensitive optical microscopy [6]. When the crystals are grown from low-pressure vapour the surface patterns occurring during growth remain virtually unchanged after the arrest of growth and subsequent cooling. In other words, artifacts due to the shutoff effect [6] are minimal. Therefore, C₆₀ is well-suited for an experimental study of crystal growth phenomena by *ex situ* surface topography.

The growth of C₆₀ crystals can be modelled quite accurately because the molecules can be regarded as spherically symmetrical; at the growth temperature the C₆₀ molecules rotate rapidly and isotropically around their centre of gravity. The interaction between the molecules is accurately described using van

der Waals forces only. This implies that only nearest and next-nearest neighbour interactions have to be considered.

The combination of experimental and theoretical accessibility makes C₆₀ grown from the vapour phase an ideal model compound for crystal growth studies. In this Letter, we present the first results of our surface studies of vapour grown C₆₀ crystals using phase sensitive optical microscopy.

2. Experimental

As starting material for crystal growth chromatographically purified C₆₀, having a purity of at least 99.95% (Syncom, the Netherlands), is used. The growth procedure has already been described in detail elsewhere [7]. In short, an evacuated quartz tube containing 6–10 mg of purified C₆₀ powder is placed in a furnace and subsequently heated to 600°C. By applying a temperature gradient of ≈ 30°C the material is transported towards the low-temperature end of the tube, after which the furnace is cooled to room temperature. Following this preparative step the major part of the tube is clean, i.e. free from possible nuclei.

The tube is subsequently heated with a constant temperature difference of 30°C between the two opposite ends of the tube, the C₆₀ originally being at the hotter end. Thus nucleation is allowed to take place at a moderate temperature and supersaturation, i.e. before the maximum temperature is reached. After

the hotter end of the tube has been at its maximum temperature of 600°C for 20 min, the furnace is gradually cooled to room temperature over 4 h. In this way good quality shiny crystals are obtained, the largest one being $0.8 \times 0.8 \times 0.8 \text{ mm}^3$ in size. The crystals have an fcc crystal structure and are bounded by $\{111\}$ and $\{100\}$ faces.

The advantage of the procedure described above is that nucleation takes place at an early stage of the process, that is at a moderate supersaturation. Because the nuclei formed act as growth centres, the supersaturation will not become very high and crystal growth occurs in a neat way. It is not possible to control the process completely, however, so the temperature at which the nucleation occurs is different for each growth run. As a consequence, the supersaturation is not the same for each growth run. These differences are clearly recognizable on the crystal surfaces (see section 3.3 below).

Some of the crystals are grown by a different procedure, in which a two-zone furnace is used. Growth takes place at 600°C at a constant temperature gradient of 20°C. The tube containing the crystals is cooled to room temperature over 6 h. In this way large crystals up to $3.5 \times 3.0 \times 1.2 \text{ mm}^3$ are obtained.

It should be mentioned that the outer layers of the crystals are deposited as the tube cools from 600°C to room temperature. Therefore the growth features on the crystal surfaces are not completely representative of the circumstances at one specific growth temperature. cooling from 600°C to room temperature results in an estimated post-growth deposition of $\approx 15 \text{ nm}$ [8]. For cooling from 400°C this is 10^{-2} nm .

The crystal surfaces are examined by optical phase contrast microscopy (PCM) and differential interference contrast microscopy (DICM) in combination with normal and high contrast photography [6]. To avoid cracking of the surfaces due to the heat introduced by illumination, low-level light intensities and a green transmission filter are used. It should be mentioned that the irradiation of the sample surface is more than one magnitude lower than the level at which polymerization occurs [9].

To minimize contamination and oxidation effects the quartz tubes containing the crystals are opened just before beginning the optical studies.

3. Observations and discussion

On the surfaces of the C_{60} crystals several features are observed. In fig. 1 the most important ones are summarized for both the $\{111\}$ and the $\{100\}$ faces. In this section we shall first discuss the post-growth phenomena observed on the surfaces (cracks and slip lines). After this, we will concentrate on the observed growth steps.

3.1. Feature

As has been reported by Haluška et al. [10] both the $\{111\}$ and the $\{100\}$ faces display cracks upon illumination. Li et al. [11] report on crack lines after

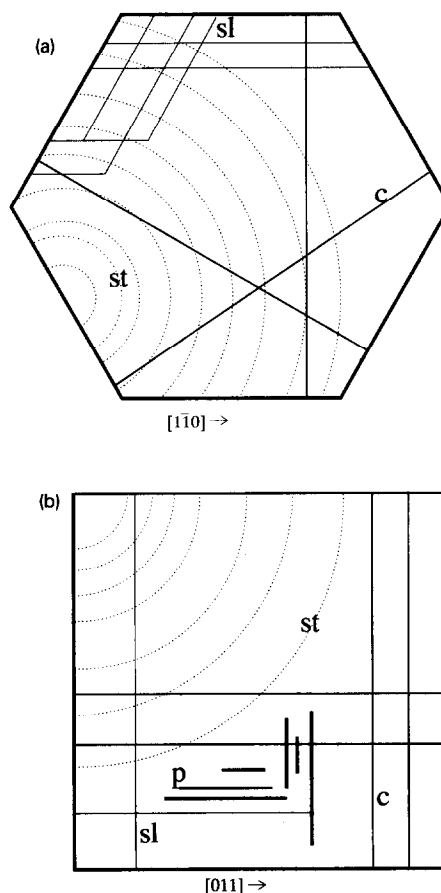


Fig. 1. Schematic showing the different phenomena observed on (a) the $\{111\}$ and (b) the $\{100\}$ surfaces; st=steps, c=cracks, sl=slip lines, p=planar faults.

indentation of the surfaces. On the $\{111\}$ faces they observe crack lines that are aligned perpendicular to the side faces, that is crack lines that propagate parallel to the $\sqrt{2}11/$ directions. On the $\{100\}$ faces their average orientation is along the diagonal directions, parallel to the $010/$ directions. In this notation, symmetrically equivalent directions h', k', l' in a given plane (hkl) are denoted as $/h'k'l'/$ [12].

On our crystals the crack lines occurring upon illumination are oriented along the $011/$ directions on the $\{100\}$ faces and along $\sqrt{2}11/$ on the $\{111\}$ faces, i.e. on both facets they are oriented perpendicular to the edges (see figs. 1 and 2a). Cracking occurs mainly at the highest magnification used, when the intensity of the incident light beam is maximal. The number of cracks depends strongly on the crystal quality. More perfect crystals, grown at low supersaturation show almost no cracking upon illumination.

Cracking occurs along those $\{110\}$ cleavage planes that are oriented perpendicularly to the crystal faces as evidenced by the observation that the cracks run parallel to the $011/$ directions on the $\{100\}$ faces and parallel to the $\sqrt{2}11/$ directions on the $\{111\}$ faces. The fact that cleavage only occurs along the perpendicular planes indicates that the thermally induced tensile or shear stresses are parallel to the surface. Otherwise the other set of $\{110\}$ cleavage planes would also have been formed, making an angle of 45° and 35° with the $\{100\}$ planes and the $\{111\}$ planes respectively.

3.2. Slip lines

On both the $\{111\}$ and the $\{100\}$ faces slip lines are commonly observed, always having a direction parallel to one of the $/110/$ directions (see fig. 1 and 2b). The slip lines thus originate from $\{111\}$ glide planes, which are typical for the dislocation movement in metal fcc lattices [13].

The majority of the slip lines cross the growth steps (section 3.3 below) without influencing the shape of the steps. Furthermore, the slip lines are perfectly straight, indicating that no further growth at the slip line (which in fact is a step) has occurred. This means that the slip lines must have been formed after cessation of crystal growth, i.e. during cooling from 600°C to room temperature. During this period a

dislocation glide is induced by a shear stresses resulting from temperature gradients in the crystal or from a difference in thermal expansion between the C_{60} and the adhering quartz wall. The slip lines often start at low angle grain boundaries, which in fact are groups of dislocations, and are restricted to the lower quality parts of the crystals. The estimated height of the slip lines ranges from ≈ 1 to 100 nm and therefore correspond with the movement of single (unit) or arrays of dislocations.

3.3. Growth steps

3.3.1. The $\{111\}$ faces

As mentioned previously, in the different growth runs different supersaturations were present, which resulted in different growth phenomena on the crystal surfaces. This section is therefore divided into two parts: first the growth phenomena observed on $\{111\}$ faces grown at low supersaturations are described and second, attention is paid to the features on faces grown at higher supersaturations.

At low supersaturation large, molecularly flat regions are found between growth steps. The steps are low: one to several nanometers high, i.e. one to a few times the monolayer thickness (see fig. 3a). The heights are estimated by comparing the contrast of the steps with that on a reference sample with known stepheights. Most of the steps are curved. Only on a few faces are slightly faceted steps found. In these cases the step edges run parallel to the periodic bond chains (PBCs) in the $/110/$ directions and are relatively high.

The steps nearly all originate from a distinct step source near of at the edge of the crystal face. On almost every face one, or a maximum of two step sources are found. In a few cases the step source is found to be in the middle of a face where the individual steps emerge from a low angle grain boundary area with many dislocation outcrops (see fig. 2b).

The occurrence of nearly all step sources near or at the edge of the face can have several reasons. One possibility is contact nucleation, in which steps are formed at the place where a neighbouring crystal is touching the face. On several crystals this effect has indeed been observed. As a large part of the crystals did not have any contacting neighbours at all, this explanation is not valid for all step sources, however.

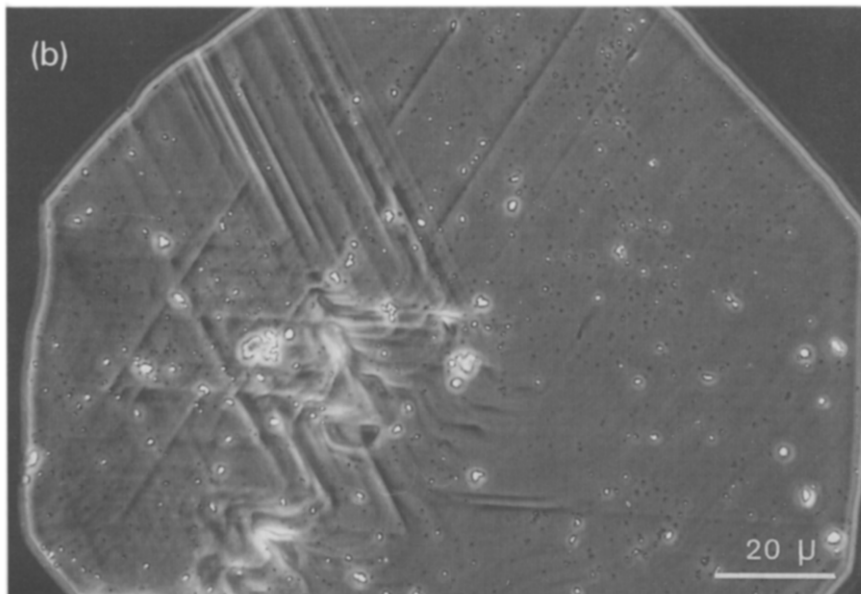
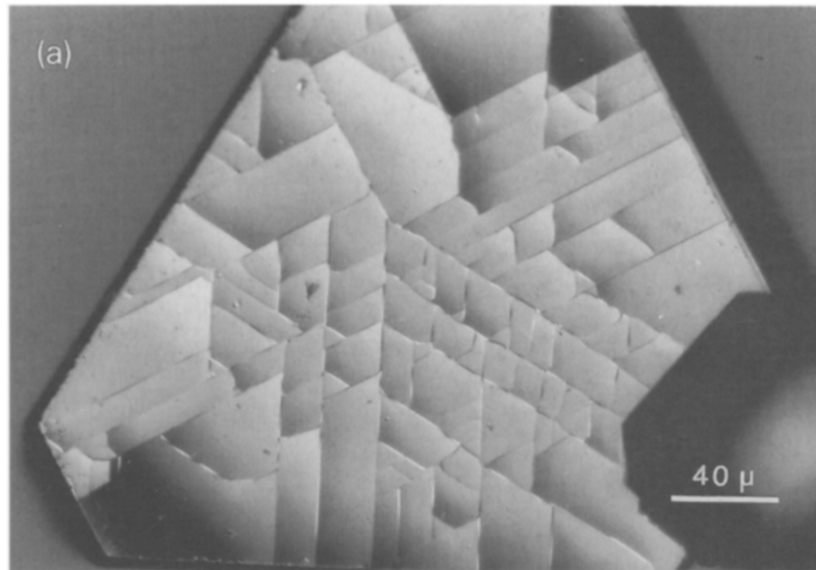


Fig. 2. Post-growth phenomena on the $\{111\}$ faces: (a) Cracks parallel to the $\langle 211 \rangle$ directions. In the upper part of the figure two exceptional cracks running in one of the $\langle 1\bar{1}0 \rangle$ directions can be seen (DICM). (b) Left half: slip lines parallel to $\langle 1\bar{1}0 \rangle$. Numerous steps emerging from a low angle grain boundary can be seen in the right half of the figure (PCM).

Another reason is that the supersaturation will be slightly higher near the edges than at the middle of the face due to volume diffusion [14]. In this case the activity, that is the number of steps generated per

unit of time, of step sources related to defects will be higher at the edges of the faces.

The distance between two neighbouring steps as well as the step shape did not change noticeably near

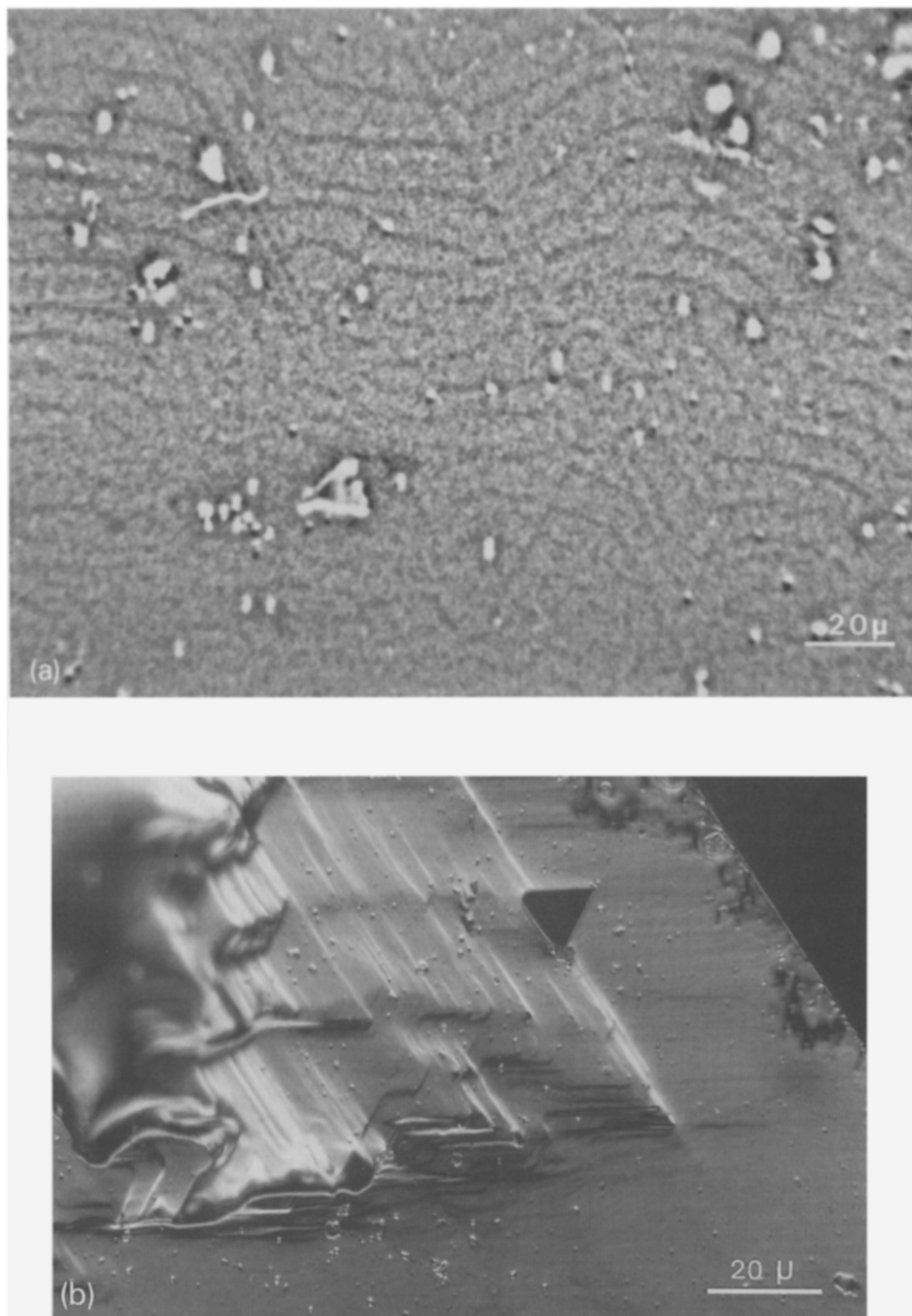


Fig. 3. Step patterns on the {111} faces: (a) Monomolecular steps and slip lines imaged by PCM followed by image processing, using unsharp masking and subsequent contrast enhancement. (b) Higher, faceted steps (DICM).

the edges of the growth faces. This indicates that in these regions the step velocity remains unaltered, so that volume diffusion must be less important than surface kinetics as a rate limiting step in crystal growth.

On surfaces grown at *higher supersaturations* a major part of the growth steps are faceted and are many monolayers high (see fig. 3b). In addition a lot of stepbunching, i.e. an accumulation of lower steps, occurs. Low, unafaceted steps have nevertheless also been observed. The steps originate from sources at or near the edge of the face, from sources at grain boundaries or from isolated points, possibly dislocation outcrops.

On some faces two-dimensional morphological instabilities are present (see fig. 4a). In this case the step edges are rough and though a certain degree of

anisotropy is present (displaying the threefold symmetry of the surface) only a small part of the saw-tooth-like step edges is faceted.

Another phenomenon observed on the $\{111\}$ faces is the occurrence of epitaxial dendrites (see fig. 4b). These dendrites have already been reported by Haluška et al. [10]. The patterns, 250 to 500 nm high as determined by optical interferometry, are present on an otherwise flat surface, which indicates that they grew while the crystal was cooling down, i.e. after the underlying crystal had been formed. Since dendrites are characteristic features of transport limited growth, it is suggested that in this case growth during cooling was limited by volume diffusion [15].

The shape of the dendrites reflects the threefold symmetry of the $\{111\}$ face, i.e. the tips are growing in the three $\sqrt{2}/3$ directions, and thus point away

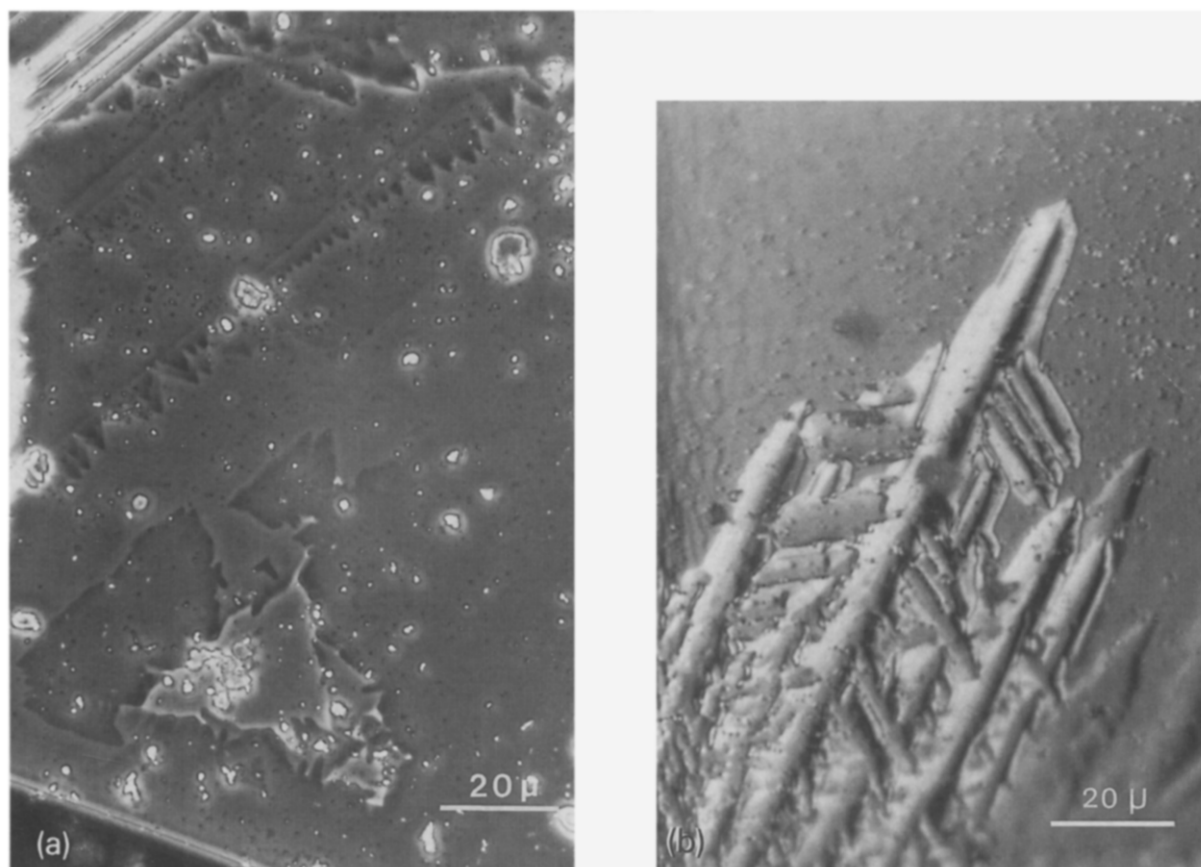


Fig. 4. Growth phenomena on the $\{111\}$ faces at higher supersaturation: (a) Morphological instabilities (PCM) and (b) epitaxial dendrites (DICM).

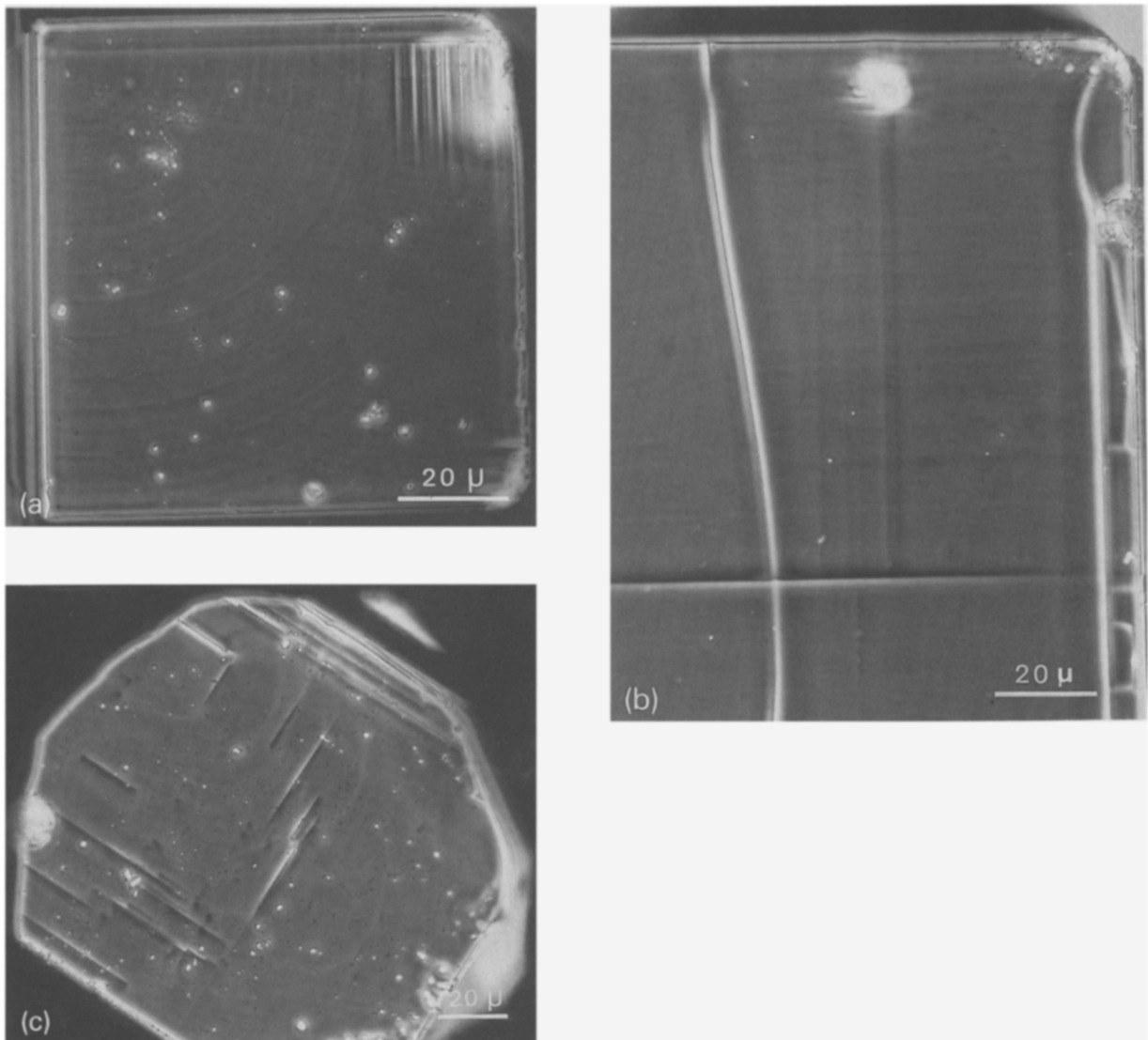


Fig. 5. Phenomena on $\{100\}$ faces (PCM): (a) A group of slip lines and low steps emerging from one growth centre. (b) Low steps emerging from a linear defect. (c) Outcrops of planar faults.

from the neighbouring $\{100\}$ faces. Note that the side branches also make an angle of 120° with the stem, obeying the threefold symmetry. Dendrite growth only occurs if in transport-limited growth there is a finite surface (step) free energy and a small lateral anisotropy in (step) growth rate. If the latter two are negligibly low then fractal or dense branching growth rather than dendrite growth takes place [16,17]. The tip of a dendrite either points towards the direction

of fastest step growth or towards the direction of lowest step free energy where the Gibbs-Thompson effect is minimal [15]. The dendrites observed in our studies point towards directions perpendicular to the PBC $/1\bar{1}0/$. This is the direction of minimal step free energy and lowest step advancement rate [18]. Therefore it can be concluded that anisotropy in step free energy rather than anisotropy in growth kinetics is decisive for the direction of epitaxial den-

write growth on the $\{111\}$ surfaces of C_{60} crystals.

3.3.2. The $\{100\}$ faces

On the $\{100\}$ faces rounded steps of varying heights are observed (see figs. 5a, 5b). If emitted from one point, the steps are circular and do not show any tendency to faceting. On crystals grown at lower supersaturations the steps are low, down to one monolayer high; at higher supersaturation they are higher. Similar to observations for $\{111\}$, on the $\{100\}$ face the steps also originate from sources near or at the edge of the face. On both the $\{111\}$ and the $\{100\}$ faces the steps are curved. This absence of anisotropy in the step patterns can be due to several reasons. First, the density of kink sites at the step edges can be independent of the orientation of the step edge. In case of step integration-limited growth the step velocity will now be isotropic. Second, surface diffusion can be the rate-limiting step in the crystal growth process. Since on the $\{111\}$ and $\{100\}$ planes with the respective two-dimensional point groups $3m$ and $4m$ the surface diffusion tensor is isotropic, the step advancement rate should also be isotropic. From our observations it cannot be concluded which of these mechanisms accounts for the isotropic step patterns.

On several faces the outcrops of planar faults are observed (see fig. 5c). They manifest themselves as straight macrosteps running parallel to the $\{011\}$ directions on $\{100\}$. Most of the fault outcrops do not end at the edges of the faces. As can be seen in fig. 5c the pattern of the growth steps is influenced by the outcrops of the planar faults. This means that these defects are already present during growth. Some of the lines even act as step sources. As their shape apparently did not change during growth they are not manifestations of glide planes. The exact nature of the defects is not known, but they can probably be assigned as stacking faults or microtwinning lamella [19]. As the outcrops are not seen on the $\{111\}$ faces the faults will most likely run parallel to the $\{111\}$ planes. Finally, on the $\{100\}$ faces we have neither observed any morphological instabilities, nor have we seen any dendrites.

4. Conclusions

Several growth and post-growth phenomena were

observed on the faces of C_{60} crystals, their presence depending on the growth conditions. On crystals grown at low supersaturations low steps down to monolayer height were observed on both the $\{111\}$ and the $\{100\}$ faces. At higher supersaturations macrosteps as well as epitaxial dendrites were found.

The treatment of the crystals after cessation of growth is of vital importance for their quality. When the crystals are cooled to room temperature rapidly, plastic deformation occurs leading to many slip lines at the surfaces. Heating the crystal surfaces with an intense light beam causes fracture of the surfaces.

The growth mechanism of C_{60} crystals is still partly unknown. We do not know which process is rate determining during crystal growth. Furthermore, the origin of the growth steps is not as yet always clear.

Vapour growth of C_{60} can be modelled relatively easily. Therefore theoretical studies of the vapour growth will be performed in the near future to solve the remaining questions.

Acknowledgement

We would like to thank P. Bennema for fruitful discussions. One of the authors gratefully acknowledges the financial support of the Netherlands Organization for Scientific Research (NWO/SON).

References

- [1] W. Krätschmer, L.D. Lamb, K. Fostiropoulos and D.R. Huffman, *Nature* 347 (1990) 354.
- [2] R.M. Fleming, A.R. Kortan, B. Hessen, T. Siegrist, F.A. Thiel, P. Marsh, R.C. Haddon, R. Tycko, G. Dabbagh, M.L. Kaplan and A.M. Muzsice, *Phys. Rev. B* 44 (1991) 888.
- [3] J.M. Hawkins, T.A. Lewis, S.D. Loren, A. Meyer, J.R. Heath, R.J. Saykally and F.J. Hollander, *J. Chem. Soc. Chem. Commun.* (1991) 775.
- [4] S.M. Gorun, K.M. Creegan, R.D. Sherwood, D.M. Cox, V.W. Day, C.S. Day, R.M. Upton and C.E. Briant, *J. Chem. Soc. Chem. Commun.* (1991) 1556.
- [5] R.M. Fleming, T. Siegrist, P.M. Marsh, B. Hessen, A.R. Kortan, D.W. Murphy, R.C. Haddon, R. Tycko, G. Dabbagh, A.M. Muzsice, M.L. Kaplan and S.M. Zahurak, *Mater. Res. Soc. Symp. Proc.* 206 (1991) 691.
- [6] W.J.P. van Enkevort, *Progr. Crystal Growth Charact.* 9 (1984) 1.
- [7] M.A. Verheijen, H. Meeke, G. Meijer, E. Raas and P. Benneman, *Chem. Phys. Letters* 191 (1992) 339.

- [8] J. Abrefah, D.R. Olander, M. Balooch and W.J. Siekhaus, *Appl. Phys. Letters* 60 (1992) 1313.
- [9] Y. Wang, J.M. Holden, Z.-H. Dong, X.-X. Bi and P.C. Eklund, *Chem. Phys. Letters* 211 (1993) 341.
- [10] M. Haluška, H. Kuzmany, M. Vybornov, P. Rogl and P. Fejdi, *Appl. Phys. A* 56 (1993) 161.
- [11] J. Li, S. Komiya, T. Tamura, C. Nagasaki, J. Kihara, K. Kishio and K. Kitazawa, *Physica C* 195 (1992) 205.
- [12] W.J.P. van Enkevort, G. Janssen, W. Vollenberg, M. Chermin, L.J. Giling and M. Seal, *Surface Coat. Technol.* 47 (1991) 39.
- [13] S. Amelinckx, in: *Dislocations in solids*, Vol. 2, ed. F.R.N. Nabarro (North Holland, Amsterdam, 1982).
- [14] A. Seeger, *Phil. Mag.* 44 (1953) 348.
- [15] J.S. Langer, *Rev. Mod. Phys.* 52 (1982) 1.
- [16] T. Viscek, ed., *Fractal growth phenomena* (World Scientific, Singapore, 1989).
- [17] E. Ben-Jacob and P. Garik, *Nature* 343 (1990) 523.
- [18] M.A. Verheijen and W.J.P. van Enkevort, to be published.
- [19] S. Muto, G. van Tendeloo and S. Amelinckx, *Phil. Mag. B* 67 (1993) 443.